

Nonstationarity of the Intraseasonal Oscillations Associated with the Western North Pacific Summer Monsoon

BIN GUAN* AND JOHNNY C. L. CHAN

Laboratory for Atmospheric Research, Department of Physics and Materials Science, City University of Hong Kong, Hong Kong, China

(Manuscript received 2 September 2004, in final form 3 August 2005)

ABSTRACT

The nonstationarity of the intraseasonal oscillations (ISOs) associated with the western North Pacific summer monsoon (WNPSM) is examined using a wavelet analysis of outgoing longwave radiation (OLR). Both the 10–20- and 30–60-day ISOs are found to display significant interannual modulations, and their relative strengths vary with time. The variation of OLR associated with a strong ISO, either 10–20- or 30–60-day, could be as large as 20 W m^{-2} in magnitude. Case studies showed that the mechanism for development of low OLR may differ in individual years, and that the 10–20-day ISO, the 30–60-day ISO, and the seasonal cycle may each become dominant in different years.

1. Introduction

Around mid-July, active convection and precipitation can be observed throughout the tropical western North Pacific (WNP; in this study, 10° – 20° N, 125° – 150° E), indicating the onset of the WNP summer monsoon (WNPSM). Several active and break periods can be observed before the withdrawal of the WNPSM. Studies have attempted to identify recurrent modes that contribute to the alternation between active and inactive periods of the Indian summer monsoon (ISM; e.g., Krishnamurti and Ardanuy 1980; Krishnamurti et al. 1985) and the South China Sea summer monsoon (SCSSM; e.g., Chan et al. 2002; Mao and Chan 2005). Generally, two components of variability were found to be dominant on an intraseasonal time scale: the “short-term” component, with a period of less than 1 month, and the “long-term” component, with a period of 1–2

months but apparently less than a season. Both can be referred to as the intraseasonal oscillations (ISOs) since they are clearly separated from the high-frequency synoptic-scale (less than 10 days) features and the slowly varying seasonal cycle as well.

Madden and Julian (1971) noticed large coherence between surface pressure, zonal winds, and temperatures at various levels over a broad period range that maximizes between 41 and 53 days. Yasunari (1979) related the eastward-propagating near-equatorial intraseasonal oscillation to active and inactive periods of the ISM. The broadband nature of this type of oscillation was emphasized by Krishnamurti and Subrahmanyan (1982), Weickmann et al. (1985), and many others, and has thereafter often been referred to as the 30–50- or 30–60-day oscillation. Murakami and Nakazawa (1985) showed that monsoon activity over an equatorial area of 50° to 150° E is directly linked to the 40–50-day oscillation via the Pacific Walker circulation. Krishnamurti and Ardanuy (1980) suggested that a phase locking between the short-term and long-term modes is responsible for producing active and break periods of summer monsoons. Though they belong to different frequency bands and shall operate in different ways, interactions may nonetheless exist in between the two types of modes. For example, Matthews and Kiladis (1999) investigated tropical–extratropical interactions

* Current affiliation: Department of Atmospheric and Oceanic Science, University of Maryland, College Park, College Park, Maryland.

Corresponding author address: Prof. Johnny Chan, Dept. of Physics and Materials Science, City University of Hong Kong, 83 Tat Chee Ave., Kowloon, Hong Kong, China.
E-mail: Johnny.Chan@cityu.edu.hk

TABLE 1. Onset date (Julian day) of the WNPSM for each year during 1975–2001 (except 1978). See section 2 for details in the definition of the onset.

Year	1975	1976	1977	1979	1980	1981	1982	1983	1984	1985	1986	1987	1988
Onset	208	198	198	203	183	158	203	218	168	168	213	188	188
Year	1989	1990	1991	1992	1993	1994	1995	1996	1997	1998	1999	2000	2001
Onset	188	168	198	228	203	183	228	198	198	253	193	183	168

between high-frequency transients and the Madden–Julian oscillation (MJO¹; Madden and Julian 1971) and showed that high-frequency waves propagating into the Indian Ocean region at the beginning of the MJO cycle might be important in the initiation of intraseasonal convective anomalies there.

The northward-propagating mode related to the ISM has been widely observed and described. Noting the similarity between the time scales of the MJO and the active–inactive–active monsoon transitions, Yasunari (1979), Julian and Madden (1981), and Lau and Chan (1986) suggested that the northward movement of convection is associated with the eastward-propagating convection along the equator. On the other hand, Wang and Rui (1990) identified a summertime mode that, as they described, moves independently to the north and may not be related to the MJO. Lawrence and Webster (2002) investigated further the relationship between the northward and eastward movements of convection for 54 individual cases of the boreal summer ISO and found that 78% of the ISOs that move northward into the Indian subcontinent also exhibit eastward movement into the western Pacific region.

The ISOs associated with the WNPSM have been relatively less described. Understanding of such ISOs needs to be improved in many aspects, including a clearer characterization of the structure and evolution of the ISOs. Strong seasonality exists for tropical ISOs in terms of their intensity, frequency, and movement (Wang and Xie 1997). Year-to-year variations may also exist especially in the context of interannual El Niño–Southern Oscillation (ENSO) variability. Specifically, mechanisms responsible for the maintenance of the WNPSM may vary among individual years. This work addresses the nonstationarity of the ISOs associated with the WNPSM on interannual time scales as manifested by outgoing longwave radiation (OLR). Data and methods are described in section 2. Sections 3 and

4 give the results from spectral and wavelet analyses, respectively. The paper concludes in section 5 with some discussions.

2. Data and methodologies

Since tropical rainfall is mostly related to convective clouds with very cold tops that emit low OLR, studies have been using the latter as a proxy of tropical rainfall. The MJO, for example, can be well observed from the OLR data. Here we used satellite observations of daily mean OLR from 1975 to 2001 (with nine months of 1978 missing) provided by National Oceanic Atmospheric Administration (NOAA; available online at <http://www.cdc.noaa.gov>; Gruber and Krueger 1984). The dataset has a spatial resolution of 2.5° latitude × 2.5° longitude with global coverage.

Daily OLR anomalies were obtained by taking out the seasonal cycle as defined by summing up the first four Fourier harmonics for any calendar year. The OLR data were then reconstructed with respect to the onset date (to be defined below) of the WNPSM. More specifically, in each year only the 3-month postonset period was retained, whereby a new multiyear dataset was formed. Noting relatively large interannual variations in the WNPSM onset date (see Table 1 and also Wu and Wang 2000), the reconstruction herein allowed for equal representation of the WNPSM by any individual year despite early, normal, or late onset in that year.

The yearly onset date was diagnosed with the summertime OLR averaged over the WNPSM domain (10°–20°N, 125°–150°E²), which requires that 1) OLR $\leq 220 \text{ W m}^{-2}$ in two consecutive pentads immediately after the onset and 2) not all the OLR in the following three pentads $> 220 \text{ W m}^{-2}$. With the above criteria, any “sustained” wet period of more than 10 days was effectively selected as the onset of the WNPSM. It should be noted that the onset dates so determined (shown in Table 1) are not unduly sensitive to the OLR

¹ As one dominant mode of tropical intraseasonal variability, the term MJO is sometimes used interchangeably with “(tropical) ISO”. In this paper, we differentiate between MJO and ISO, with MJO being a synonym to tropical 30–60-day oscillation, while ISO a more general term not implicit of any specific frequency band.

² The WNPSM domain used here is accurate to the extent that it is representative. The readers are referred to other studies (e.g., Zeng and Lu 2004) for a careful definition of monsoon domains.

threshold, nor are the subsequent analyses, as a result. While it is not the focus of this note to discuss in detail the formulation and validation of the onset criteria, a quick comparison with Zeng and Lu (2004) and references therein showed broad consistency in the onset dates respectively determined, that is, the *entire* WNPSM domain enters the summer monsoon period around the 40th Julian pentad (or 196th–200th Julian day) climatologically. The consistency between our OLR-based and their precipitable-water-based onset criteria may be attributed to the geographical location of the WNPSM; as a known fact, the relationship between OLR and precipitation is strong over tropical oceans.

Spectral analysis was used to identify the dominant ISOs. For any time series, a quick estimate of the power spectrum could be the squared Fourier transform, which however could be misleading as a result of power leakage. One of the remedies to this is the so-called “multitaper method” (MTM; Mann and Lees 1996). The idea is to apply a set of “tapers” (windows) to the time series and then average the tapered spectrum over all the tapers. Sometimes climate time series may consist of a variety of frequency regimes that are localized in time (such as the OLR time series to be analyzed in this study), in which case wavelet analysis/transform (e.g., Torrence and Compo 1998) is a useful tool to investigate the power spectrum in both frequency and time domain. Mathematically, wavelet transform is nothing but the convolution of the time series and some wavelet function specified by the so-called “wavelet scale” and time position. By varying the wavelet scale and time position, one can then construct a two-dimensional picture showing how the wavelet power varies in frequency and in time. Lanczos bandpass filters (Duchon 1979) were used to obtain the OLR associated with the ISOs. Cutoff frequencies were selected based on the spectral analysis in section 3. The number of weights used was 721, with which the Gibbs phenomenon was hardly discernable (not shown).

3. Dominant ISOs in the WNPSM

So far little consensus exists as to where the various ISOs locate in frequency space. Often referred to are 10–20- and 30–60-day oscillations, while variants are not uncommon (e.g., Kiladis and Weickmann 1992; Matthews and Kiladis 1999; Wang and Xie 1997; Lawrence and Webster 2002). The diversity in terminology itself is circumstantial evidence of the lack of a good understanding, probably due to large variations in the properties of the ISOs with respect to time and/or geographical locations.

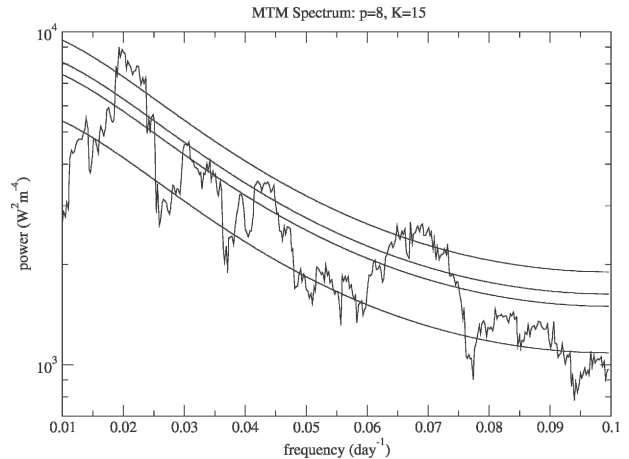


FIG. 1. MTM spectrum (Mann and Lees 1996) of the WNPSM OLR (i.e., area-averaged reconstructed OLR over 10° – 20° N, 125° – 150° E, the WNPSM domain; see section 2 for details in OLR reconstruction); $p = 8$ and $K = 15$. The four smooth curves, from bottom to top, indicate the median, 90%, 95%, and 99% significance levels, respectively.

To identify the dominant climatological ISOs associated with the WNPSM, a spectral analysis is performed on the reconstructed OLR averaged over the WNPSM domain (10° – 20° N, 125° – 150° E; hereafter the WNPSM OLR) using the multitaper method (see section 2 for details in data preparation and a brief description of the method). It should be noted that near the center of the WNPSM domain, the area averaging is not necessary (not even a nine-cell smoothing) to obtain similar spectral peaks to be discussed.³ Two spectral peaks, centered at the period of about 15 and 45 days, respectively, stand out clearly from the assumed red noise background at the 99% significance level (Fig. 1). This is especially true for the lower-frequency one, its power being well above neighboring frequencies. If the 95% significance level is used, a third peak will be observed on the 22–25-day band. Another spectral analysis using the Blackman–Tukey method (Kay 1988) as well as a time-averaged wavelet analysis (not shown) reproduced only the 15- and 45-day-centered peaks, which raises doubt about the real significance of the 22–25-day peak.

4. Nonstationarity of the dominant ISOs

Implicit in the spectral analysis in section 3 is an assumption of stationarity of the time series. This is con-

³ Note, however, that this becomes less true when moving eastward away from the center of the WNPSM domain. Specifically, the 30–60-day ISO becomes weaker and less significant farther to the east.

venient to provide a climatological overview, with possible time dependencies intentionally ignored. In this section, wavelet analysis (see section 2 for a brief description) is used to search for time periods when these ISOs are relatively strong/weak, and, in each case, how the low OLR in WNPSM is realized. The OLR time series being analyzed is the same as in section 3, that is, the WNPSM OLR.

a. Overview

The time-averaged wavelet spectrum (not shown) shows consistent features with the MTM spectrum, with two spectral peaks centered at the period of 10–20 and 30–60 days, respectively. Some interesting features are found with the time series of the wavelet power averaged in frequency space for the two types of ISOs (Fig. 2). The selection of the two frequency bands for averaging is based on the spectral analysis in section 3 (and one other cross-validating analysis). Both the 10–20- and 30–60-day modes, as seen, display significant modulation in amplitude in certain years. Also, the relative strengths of the two vary with time. For the 30–60-day mode, substantially strong power is observed during 1977–79⁴ and 1983–85. Moderately strong power is also observed during 1996. During these years, the 30–60-day mode dominates over the 10–20-day mode in strength. On the other hand, there are two periods in 1981 and 1993 when the power of the 10–20-day mode becomes overwhelmingly high. Also observed are two periods when both two modes are inactive, that is, 1990–91 and 1997–98. It is of interest to note that the years of 1991 and 1997 each feature a strong El Niño event. Possible relationship between interannual variability of the WNPSM onset and ENSO has been discussed in previous studies (e.g., Ueda and Yasunari 1996; Wu and Wang 2000). Noteworthy here is that, in addition to the onset variability, the WNPSM may manifest interannual variability in many aspects, such as the type and strength of the dominant ISO and its relative importance to the seasonal cycle.

b. Case studies

We have identified periods when either the 10–20- or 30–60-day ISO is relatively strong. It is of interest to zoom in on the OLR variations on the respective frequency bands during these time periods. Presented be-

low are the results for two representative years, namely, 1981 when the 10–20-day ISO is relatively strong and 1984 when the 30–60-day ISO is relatively strong.

In general, the WNPSM is characterized by northward (and westward; not shown) propagation of the 10–20- or 30–60-day ISO, whichever is stronger (Fig. 3). The dominant ISO maintains its strength during the 3-month period after the onset of WNPSM. The 30–60-day ISO has its origin in the deep Tropics, while the 10–20-day ISO is more confined latitudinally to within 10°–20°N. Zonally, the 10–20-day ISO propagates westward from almost as east as the date line, while the 30–60-day ISO—also propagating westward—is essentially restricted to westward of 150°E (not shown). The OLR variations associated with the dominant ISO have magnitudes of over 20 W m⁻², comparable in strength to the variations one might expect from the seasonal cycle. Conceivably, a synchronization of the dominant ISO to the seasonal cycle could generate OLR anomalies twice as strong as either could do individually. However, this mechanism of attaining minimum OLR does not appear to be in operation at least for the three cases to be shown below.

The relationship between the ISOs and the seasonal cycle are further examined in terms of their relative roles in generating low OLR in WNPSM (shown in Fig. 4). The seasonal cycles in 1981 and 1984 both have much smaller magnitude if compared to the respective dominant ISO in each year, with the dominant ISO being responsible for the alternation between high and low OLR. In 1990, alternatively, the seasonal cycle overwhelms the ISOs in strength, with the former being the dominant component that characterizes the development of low OLR in WNPSM after the onset.

5. Summary and discussion

This note emphasizes the nonstationarity of the ISOs associated with the WNPSM. It is found that either of the two dominant ISOs, 10–20- or 30–60-day, displays significant modulation in time. Two periods, that is, 1977–79 and 1983–85, are found to have substantially strong power on the 30–60-day band. On the other hand, the years of 1981 and 1993 are characterized by predominant power on the 10–20-day band. Besides, there are two periods, that is, 1990–91 and 1997–98, during which both of the two ISOs are inactive. It is of interest to note that 1991–92 and 1997–98 are both El Niño winters, and the following summers each feature a late WNPSM onset (see Table 1). Another two late onsets are observed to be following the El Niño winters of 1982/83 and 1994/95, respectively. On one hand, it

⁴ Note that the year 1978 was actually not included in the analysis because of data incompleteness. Strong power is inferred for the year 1978 on the 30–60-day band considering the continuously increasing power in the previous year and decreasing power in the following year, which however remains to be validated.

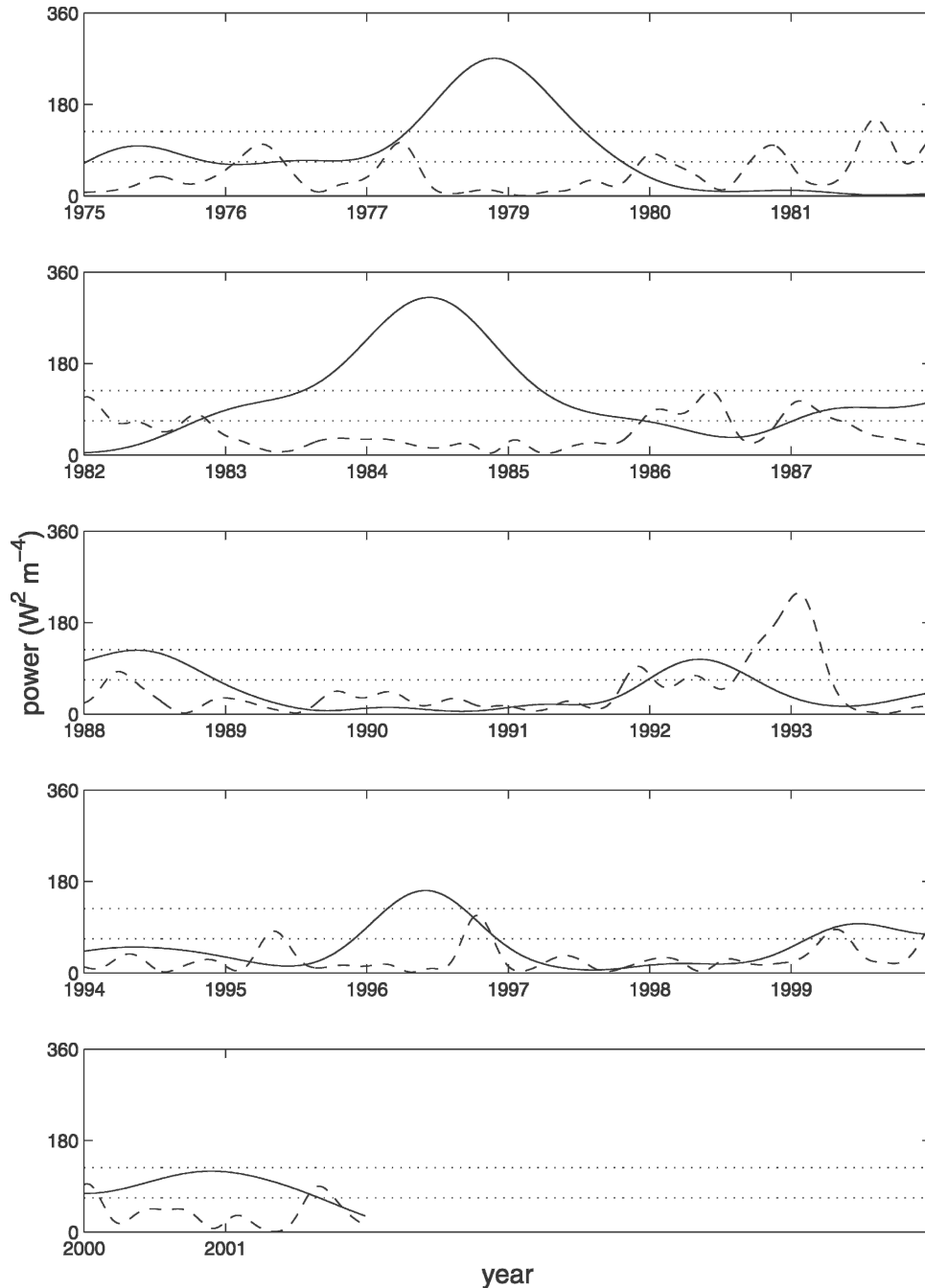


FIG. 2. The 30–60-day (solid) and 10–20-day (dashed) scale-averaged Morlet wavelet spectrum (Torrence and Compo 1998) of the WNPSM OLR (the same OLR time series as used in Fig. 1), with the 95% significance levels indicated by the upper (for 30–60 days) and lower (for 10–20 days) dotted lines, respectively. Note that the year 1978 was omitted because of incomplete data.

appears that late WNPSM onsets tend to occur during the decaying phase of ENSO, which is consistent with the findings of Wu and Wang (2000). On the other hand, the relationship between the onset timing and strengths of the ISOs remains unclear, that is, early

(late) onsets are not necessarily accompanied by strong (weak) ISOs, and vice versa. Wu and Wang (2000) attributed large interannual variations in the WNPSM onset to the varying seasonal cycle, with contributions from the ISO of secondary importance; the argument

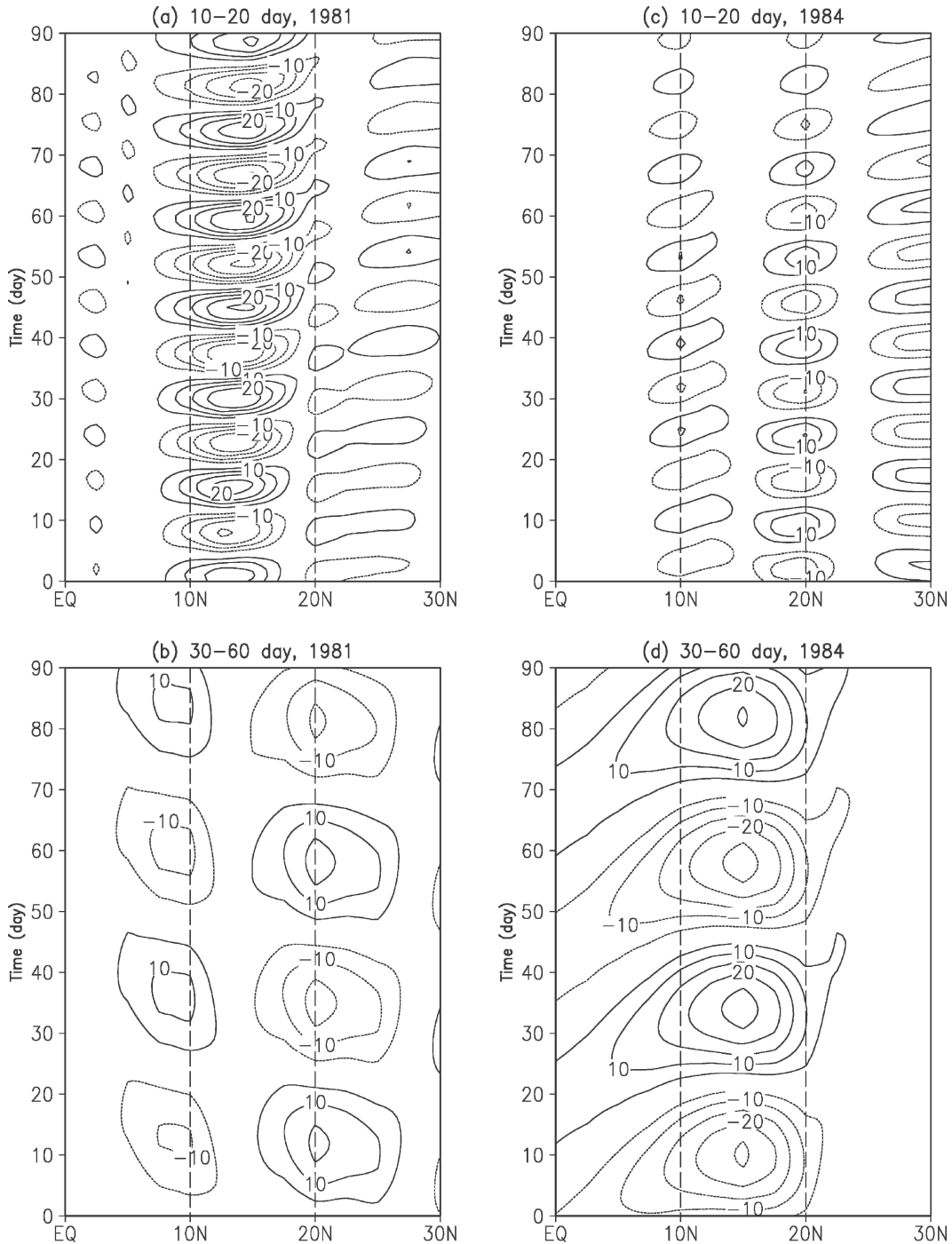


FIG. 3. Time–latitude sections of Lanczos bandpass-filtered OLR (W m^{-2}) at 137.5°E . Refer to labels on top of each panel for filtering bands and calendar years. Positive (negative) values are solid (dashed), and zero contours are omitted. The vertical dashed lines indicate the latitudinal domain for the WNPSM. The time axis is labeled in number of days after the onset of WNPSM. Contour interval: 5 W m^{-2} . Note that labels are drawn on every other contour.

could however be an artifact of not distinguishing between the two types of ISOs.

It is found that the mechanism for development of low OLR in WNPSM may differ in individual years.

Specifically, we found with case studies that the 10–20-day ISO, the 30–60-day ISO, and the seasonal cycle are predominantly important for the years 1981, 1984, and 1990, respectively. The 10–20-day ISO has its origin in

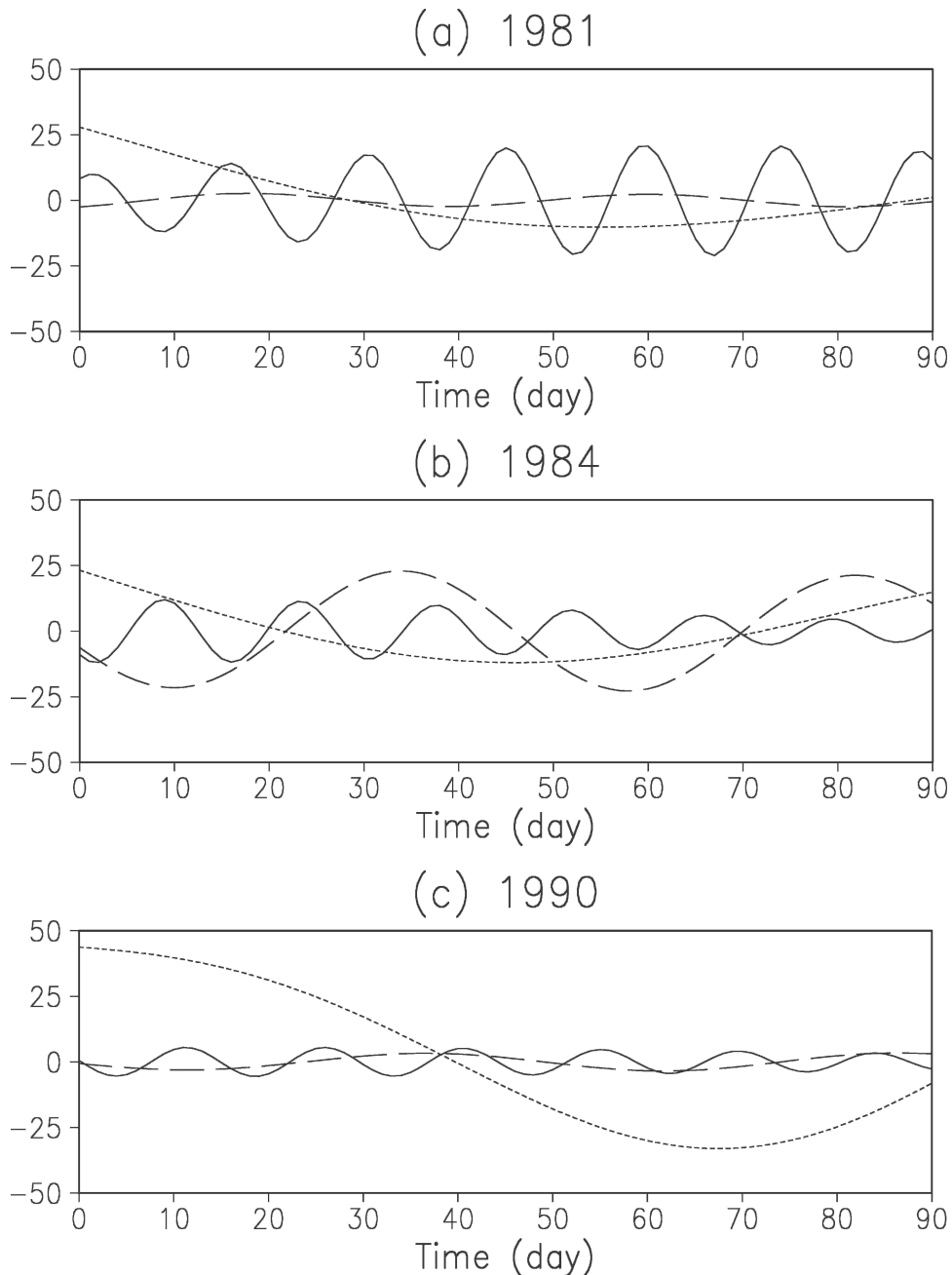


FIG. 4. Time series of OLR (W m^{-2}) averaged over the WNPSM domain (10° – 20°N , 125° – 150°E) for the 10–20-day ISO (solid), the 30–60-day ISO (long dashed), and the seasonal cycle (short dashed). Lanczos bandpass filters were used to obtain the ISOs. The seasonal cycle was obtained by summing up the first four Fourier harmonics of the OLR time series for any calendar year. Refer to labels on top of each panel for calendar years. The time axis is labeled in number of days after the onset of WNPSM.

equatorial central Pacific and propagates northwestward, which is reminiscent of atmospheric response to anomalous heating in the Tropics (Matsuno 1966; Gill 1980). The 30–60-day ISO emanates from deep Tropics and may therefore be related to MJO propagation.

Aside from possible mechanisms for generating the various ISOs, the interannual variations thereof should—noting the results herein—also be further investigated for a more complete picture of the WNPSM and its variability.

Acknowledgments. The authors acknowledge the use of the SSA-MTM Toolkit provided by the UCLA SSA-MTM group from their Web site (<http://www.atmos.ucla.edu/tcd/ssa/>), and the Matlab wavelet scripts provided by Christopher Torrence and Gilbert P. Compo from their Web site (<http://paos.colorado.edu/research/wavelets/>). Comments and suggestions from two anonymous reviewers have been helpful to the improvement of the original manuscript. The work of the first author forms part of his M.Phil. research, which is supported by a Postgraduate Studentship from the City University of Hong Kong. This research is partially supported by City University of Hong Kong Strategic Research Grant 7000010.

REFERENCES

- Chan, J. C. L., W. Ai, and J. Xu, 2002: Mechanisms responsible for the maintenance of the 1998 South China Sea summer monsoon. *J. Meteor. Soc. Japan*, **80**, 1103–1113.
- Duchon, C. E., 1979: Lanczos filtering in one and two dimensions. *J. Appl. Meteor.*, **18**, 1016–1022.
- Gill, A., 1980: Some simple solutions for heat-induced tropical circulation. *Quart. J. Roy. Meteor. Soc.*, **106**, 447–462.
- Gruber, A., and A. F. Krueger, 1984: The status of the NOAA outgoing longwave radiation data set. *Bull. Amer. Meteor. Soc.*, **65**, 958–962.
- Julian, P. R., and R. A. Madden, 1981: Comments on a paper by T. Yasunari: A quasistationary appearance of 30- to 40-day period in the cloudiness fluctuations during the summer monsoon over India. *J. Meteor. Soc. Japan*, **59**, 435–437.
- Kay, S. M., 1988: *Modern Spectral Estimation—Theory and Application*. Prentice-Hall, 543 pp.
- Kiladis, G. N., and K. M. Weickmann, 1992: Circulation anomalies associated with tropical convection during northern winter. *Mon. Wea. Rev.*, **120**, 1900–1923.
- Krishnamurti, T. N., and P. Ardanuy, 1980: The 10- to 20-day westward propagating mode and “breaks in the monsoons.” *Tellus*, **32**, 15–26.
- , and D. Subrahmanyam, 1982: The 30–50-day mode at 850 mb during MONEX. *J. Atmos. Sci.*, **39**, 2088–2095.
- , P. K. Jayakaumar, J. Sheng, N. Surgi, and A. Kumar, 1985: Divergent circulation on the 30 to 50 day time scale. *J. Atmos. Sci.*, **42**, 364–375.
- Lau, K.-M., and P. H. Chan, 1986: Aspects of the 40–50 day oscillation during the northern summer as inferred from outgoing longwave radiation. *Mon. Wea. Rev.*, **114**, 1354–1367.
- Lawrence, D. M., and P. J. Webster, 2002: The boreal summer intraseasonal oscillation: Relationship between northward and eastward movement of convection. *J. Atmos. Sci.*, **59**, 1593–1606.
- Madden, R. A., and P. R. Julian, 1971: Description of a 40–50 day oscillation in the zonal wind in the tropical Pacific. *J. Atmos. Sci.*, **28**, 702–708.
- Mann, M. E., and J. M. Lees, 1996: Robust estimation of background noise and signal detection in climatic time series. *Climate Change*, **33**, 409–445.
- Mao, J., and J. C. L. Chan, 2005: Intraseasonal variability of the South China Sea summer monsoon. *J. Climate*, **18**, 2388–2402.
- Matsuno, T., 1966: Quasi-geostrophic motions in the equatorial area. *J. Meteor. Soc. Japan*, **44**, 25–43.
- Matthews, A. J., and G. N. Kiladis, 1999: The tropical–extratropical interaction between high-frequency transients and the Madden–Julian oscillation. *Mon. Wea. Rev.*, **127**, 661–677.
- Murakami, T., and T. Nakazawa, 1985: Tropical 45 day oscillation during the 1979 Northern Hemisphere summer. *J. Atmos. Sci.*, **42**, 1107–1122.
- Torrence, C., and G. P. Compo, 1998: A practical guide to wavelet analysis. *Bull. Amer. Meteor. Soc.*, **79**, 61–77.
- Ueda, H., and T. Yasunari, 1996: Maturing process of the summer monsoon over the western Pacific—A coupled ocean/atmospheric system. *J. Meteor. Soc. Japan*, **74**, 493–508.
- Wang, B., and H. Rui, 1990: Synoptic climatology of transient tropical intraseasonal convection anomalies: 1975–1985. *Meteor. Atmos. Phys.*, **44**, 43–61.
- , and X. Xie, 1997: A model for the boreal summer intraseasonal oscillation. *J. Atmos. Sci.*, **54**, 72–86.
- Weickmann, K. M., G. R. Lussky, and J. E. Kutzbach, 1985: Intraseasonal (30–60 day) fluctuations of outgoing longwave radiation and 250 mb stream function during northern winter. *Mon. Wea. Rev.*, **113**, 941–961.
- Wu, R., and B. Wang, 2000: Interannual variability of summer monsoon onset over the western North Pacific and the underlying processes. *J. Climate*, **13**, 2483–2501.
- Yasunari, T., 1979: Cloudiness fluctuations associated with the Northern Hemisphere summer monsoon. *J. Meteor. Soc. Japan*, **57**, 227–242.
- Zeng, X., and E. Lu, 2004: Globally unified monsoon onset and retreat indexes. *J. Climate*, **17**, 2241–2248.